

Soluble TAM receptor AXL triggers changes in cell behavior and signaling of bladder cancer cells

Student: Almira Kaliyeva

Supervisor: Marina Kriajevskaia, PhD

Bachelor of Medical Sciences
Nazarbayev University School of Medicine

Astana, 2023

I hereby declare that the Capstone project is my original work, and it has been written by me in its entirety. I have duly acknowledged all the sources of information that have been used in the Capstone project. In addition, this Capstone project has also not been submitted for any degree in any university previously.

Abstract

AXL, a member of the TAM family, has emerged as a potential target for treating bladder cancer due to its role in cellular activities and tumorigenesis. This receptor was found to be overexpressed in cancer. Here, the soluble form of AXL (sAXL) is studied. sAXL has been proposed to act as a decoy receptor, which sequesters growth arrest-specific 6 (Gas6) ligand and shuts down Gas6/AXL axis. This hypothesis has been supported by several studies that demonstrated a high-affinity binding between sAXL and Gas6. Nevertheless, the role of sAXL in cellular signaling in bladder cancer has not been studied. This study investigated if sAXL affects cell behavior and signaling of bladder cancer cells and if it can act as a decoy. The recombinant AXL and Gas6 were used for the analysis, and cells were cultured with further incubation with these proteins. Western blotting was used to investigate the expression of AXL downstream targets. The findings revealed that sAXL has a similar effect on cells as Gas6, proposing that sAXL may participate in homophilic and heterophilic binding with TAM receptors. Moreover, sAXL sequestered Gas6 in pAkt-308 activation. As a future perspective, a broader analysis of the interactions between soluble AXL and TAM receptors is needed.

Introduction

Bladder cancer

Bladder cancer is the 10th most frequently diagnosed cancer, with over 500,000 annual diagnoses and 200,000 annual deaths worldwide. Among males, bladder cancer is the leading cause of cancer deaths, with an incidence of 9.6 and a mortality rate of 3.2 per 100,000 men, respectively (Sung et al., 2021).

The bladder is an organ in the lower abdomen that primarily functions as a storage reservoir for urine received from the kidneys until micturition. The urinary bladder and urinary tract are lined by urothelial cells responsible for urine accommodation. After filtration, these cells are frequently exposed to potential mutagenic agents found in the urine (Saginala et al., 2020). Cancer originating from the urothelial cells is called urothelial carcinoma, accounting for 90% of all bladder cancer cases (Dougherty et al., 2009). Urothelial carcinoma is further subclassified into non-muscle invasive (NMI) and muscle-invasive (MI) bladder cancers. Muscle-invasive or metastatic bladder cancer is initially diagnosed in roughly 25% of patients with bladder tumors, while NMI bladder cancer accounts for approximately 75% of new diagnoses (Kamat et al., 2016).

The development of bladder cancer is a complex process influenced by different risk factors such as sex, age, genetic predisposition, occupational exposure, pollution, and lifestyle. Among the various environmental factors, tobacco smoking is the major contributor to bladder cancer occurrences. Despite advancements in treatment options such as robotic surgical methods, radiation, and chemotherapies, their effectiveness is still unclear (Dreicer, 2017 & Sung et al., 2021). Moreover, diagnosis of bladder cancer continues to be done via the golden standard procedures such as cystoscopy and urinary cytology (Oliveira et al., 2020). The high invasiveness of cystoscopy and low sensitivity of cytology highlight the need for further research into more effective and novel diagnostic approaches, such as identifying urinary biomarkers.

Receptor Tyrosine Kinases

Over the past decades, studies on the molecular biology of bladder cancer found multiple alterations in receptor tyrosine kinases to be commonly engaged in bladder malignancies (Martin-Doyle & Kwiatkowski, 2015). Receptor tyrosine kinases are a large family of proteins responsible for controlling cell-to-cell communication and a diverse range of biological functions (Karl et al., 2022). Human RTKs have the same molecular structure: an extracellular domain, a helical transmembrane domain, and an intracellular tyrosine kinase domain (Lemmon & Schlessinger, 2010). These receptors are mainly involved in the phosphorylation of multiple tyrosines and have a critical role in intracellular activities such as proliferation, survival, migration, and resistance to the therapy (Abboud-Jarrous et al., 2017). For these cell processes being of utmost importance, RTK's enzymatic functions are strictly regulated. The abnormal function of RTKs leads to an assortment of different human diseases, including cancer (Du & Lovly, 2018). Specifically, in various tumors like bladder cancer, RTKs are upregulated and are linked to accelerated tumor proliferation and progression. Therefore, targeting RTKs is a promising approach to cancer treatment (Zangouei et al., 2020).

TAM receptors

This study focuses on the TAM family of RTKs, which is overexpressed in various types of cancer, such as breast, lung, ovarian, and prostate cancer. It is also associated with poor prognosis and resistance to chemotherapy and radiation therapy (Lemke, 2013). However, studies on TAM receptors in bladder malignancies are still limited.

According to Wu et al. (2014), TYRO3, AXL, AND MER are members of the TAM family which are encoded by three different genes situated on chromosomes 15q15, 19q13.2, and 2q14.1, respectively. TAM receptors are single-pass transmembrane receptors, all carrying a catalytically competent protein-tyrosine kinase. The extracellular domains of these receptors carry tandem fibronectin type III repeats and tandem immunoglobulin-related domains responsible for ligand binding (Lemke, 2013).

Activation of TAM receptors is initiated by binding a specific ligand that triggers their dimerization and autophosphorylation of specific tyrosine residues which is dependent on the presence of ATP (Verma et al., 2011). Protein S (PROS1) and Growth Arrest-Specific 6 (GAS6) are two important ligands that activate the TAM family members. Both ligands are the vitamin K-dependent protein family members (Hafizi & Dahlbäck, 2006a). GAS6 can interact with all TAM family receptors, while PROS1 can bind TYRO3 and MER only (Lew et al., 2014). Nonetheless, a recent investigation has provided evidence that PROS1 can activate AXL in glioma spheroids (Sadahiro et al., 2018).

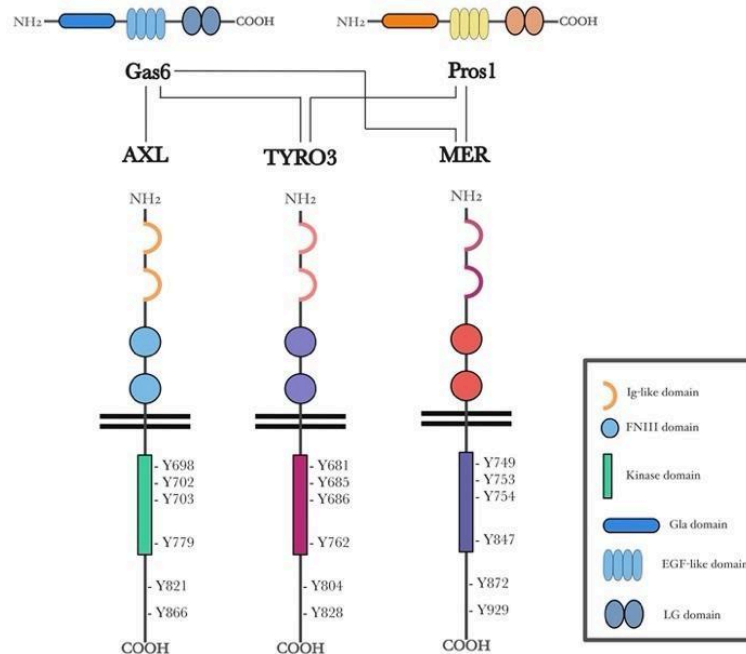


Figure 1. A scheme illustrating the structure of TAM receptors and their ligands. Tyrosine phosphorylation sites within kinase and distal cytoplasmic regions are shown. Thin lines show ligand specificity to receptors. *Note.*

Created with Vertinator.

AXL receptor: discovery

Among this family, AXL has received significant attention. Its discovery dates back to 1988 when researchers searched for transforming genes in patients who had chronic myeloid and

developed a condition called ‘blast crisis’ (Liu et al., 1988). In 1991, two separate research groups characterized AXL. O’Bryan et al. (1991) discovered an overexpressed cDNA of leukemic cells, which they called AXL, meaning uncontrolled, from the Greek word ‘anexelekto’ (Rankin et al., 2010). In a separate study, Janssen and colleagues (1991) identified the same transforming cDNA in NIH/3T3 cells transfected with DNA from a patient with a chronic myeloproliferative disorder. It was called UFO, indicating its unknown function. Both cDNAs were found to encode a new 140 kDa receptor tyrosine kinase, which was named AXL. Since then, AXL has gained considerable attention as a potential target for anticancer therapies and is also a focus of this study.

According to studies conducted by O’Bryan et al. (1991), the human *axl* gene is situated on chromosome 19, band q13.2, and encodes 20 exons. The extracellular region (exon 1-10) of the transmembrane protein juxtaposes two immunoglobulin-like domains and two fibronectin type III repeats. The intracellular region (Exon 12-20) of AXL has three tyrosine residues, namely Y779, Y821, and Y866 (Hafizi & Dahlbäck, 2006b). Alternative splicing of exon 10 leads to the production of two different isoforms, long and short, both of which are implicated in cancer (O’Bryan et al., 1991).

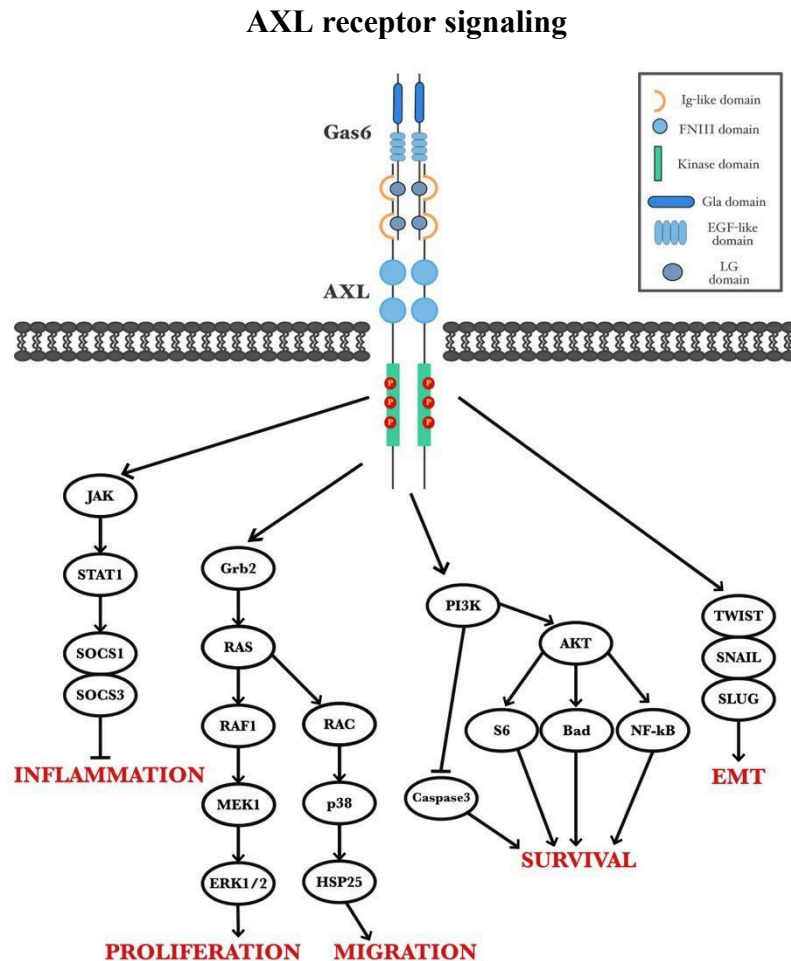


Figure 2. Illustration of AXL receptor-mediated signaling pathways. AXL receptor is activated upon binding to Gas6. Arrows show signal transduction; thin lines indicate inhibition. *Note.* Created with Vertinator.

AXL has emerged as a crucial regulator of multiple signaling pathways involved in cell growth, proliferation, and survival (Figure 2). The activation of the AXL receptor involves binding

with its ligand, GAS6, leading to dimerization and cross-phosphorylation. This process begins with GAS6 binding AXL to form GAS6/AXL complex, followed by autophosphorylation at tyrosine residues Y779, Y821, and Y866 (Pacez et al., 2013). The activated AXL receptor then triggers critical signaling pathways such as PI3K/Akt and MAPK, which are implicated in cell survival and proliferation. For instance, in breast cancer cells, AXL activation has been linked to the upregulation of MAPK activation, resulting in increased cell invasion and migration (Asiedu et al., 2014). Similarly, AXL has been shown to upregulate the Akt pathway, promoting resistance to chemotherapy (Wang et al., 2016). Moreover, AXL signaling regulates genes implicated in the epithelial-mesenchymal transition (EMT), a process by which epithelial cells acquire mesenchymal properties, promoting their migration and invasion into surrounding tissues (Gjerdrum et al., 2010). Overexpression of AXL is known to be driven by an EMT-associated transcriptional program, as confirmed by various studies (Antony & Huang, 2017).

Soluble AXL

The full-length AXL protein has a soluble form called sAXL, which lacks the transmembrane and cytoplasmic domains but retains the ligand-binding domain capable of interacting with Gas6 and competing with the membrane-bound AXL. Budagian et al. (2005) and Miller et al. (2016) showed that a soluble form of AXL is a product of proteolytic cleavage by a disintegrin-like metalloproteinase (ADAM)10 and ADAM17. Numerous studies regarding the full transmembrane AXL protein have provided extensive knowledge of the biological and clinical functions of the receptor. Meanwhile, the role of sAXL in biological processes is not yet thoroughly studied but has attracted researchers' attention in recent years.

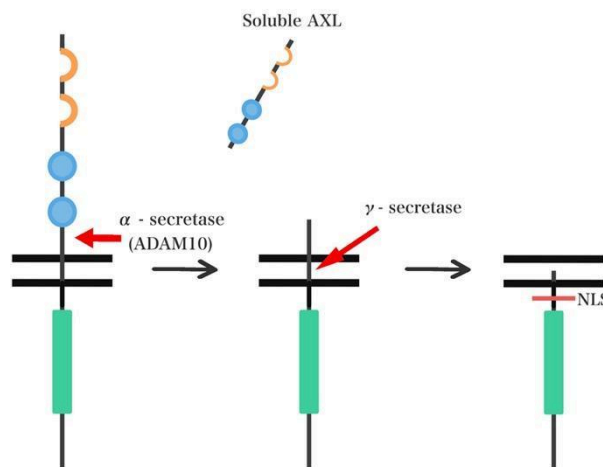


Figure 3. Model of proteolytic cleavage of the AXL RTK. The receptor is processed by α -secretase (ADAM10/ADAM17) and γ -secretase. The cleavage product of the α -secretase is the soluble form of AXL which retained Ig-like domains and FNIII repeats, and the product of γ -secretase translocates into the nucleus by a nuclear localization signal (NLS). *Note.* Created with Vertinator.

sAXL levels have been found to increase in various pathologies, such as cancer, heart failure, and some inflammatory conditions (Martínez-Bosch et al., 2022). Additionally, the shed ectodomain is overexpressed in malignant effusions but is lowered after exposure to chemotherapy (Flem-Karlsen et al., 2020). Thus, sAXL has been reported as a potential biomarker for the early detection of certain types of cancer that could improve prognosis and treatment (Martínez-Bosch et

al., 2022). It has been proposed to function as a decoy receptor that binds GAS6, leading to AXL signaling shutdown and preventing GAS6-induced mitogenic effects. As an engineered decoy receptor, sAXL demonstrated promising results in decreasing metastatic potential in animal models (Kariolis et al., 2014 & Zhu et al., 2019). Hence, there is a growing interest in sAXL as a potential target in cancer.

Despite the received attention in research, the role of soluble AXL in bladder cancer is still undefined and requires further investigation. This study aims to examine how the proteolytically cleaved fragments of AXL (sAXL) influence the behavior and signaling of bladder cancer cells. This research also investigates whether sAXL stimulates or inhibits downstream signaling. It is hypothesized that soluble AXL acts as a decoy receptor to Gas6.

Materials and Methods

Cell Culture

Cell lines

The bladder cell lines J82 and HT1376 were obtained from the American Type Culture Collection (ATCC, Manassas, VA, USA).

Table 1. Characteristics of cell lines

Cell lines	Phenotype	Characterization	AXL expression
J82	Mesenchymal	Sex of cell: Male Age at sampling: 58Y Disease: Bladder carcinoma	positive on AXL
HT1376	Epithelial	Sex of cell: Female Age at sampling: 58Y Disease: Bladder carcinoma	negative on AXL

Cell thawing

Frozen vials of cells were obtained from the -80°C fridge. Cells were warmed up directly in the hands. 1 mL of the cell suspension was transferred into the 15 mL tube with 4 mL of the complete media. The tube was then spun down at 1000 rpm for 5 minutes. After that, the supernatant was discarded, and the pellet was resuspended in 1 mL of a new media. Cells were cultured in T25 flasks.

Cell culture and supplements

Cell culture procedures were carried out under sterile conditions in a tissue culture hood, and cells were maintained in an incubator at 37°C with 5% CO₂. Bladder cancer cells were cultured in RPMI 1640 Medium, with L-Glutamine obtained from CAPRICORN Scientific. Media was adjusted to contain 10% Fetal Bovine Serum (FBS) (Sigma, F9665), 1% of Penicillin-Streptomycin (Sigma-Aldrich, P0781-100 ml), 1% of non-essential amino acids (GIBCO, 11140-035), and 1% Sodium Pyruvate.

Cell passaging

Cells were passaged once they had reached 70-80% confluency. It was performed by discarding the old media, washing cells with 1xPhosphate-Buffered Saline (PBS) purchased from GIBCO 18912-014, and incubating cells with 1xTrypsin (CAPRICORN Scientific, TRY-2B10) at 37°C for 3 minutes to dissociate adherent cells from surfaces. The cells were then resuspended in a 15 mL falcon tube with the complete medium. The tube was spun at 1000 rpm for 5 minutes. The media was removed, and the pellet was resuspended in 1 mL of a new media. Cells were added dropwise on the entire surface of the T75 flask with 14 mL of fresh media prepared in advance. Cells were then transferred to the 37°C CO₂ incubator.

Cell freezing

Cells were grown in T75 flasks reaching 80% confluency. The old media was aspirated, and cells were washed with 1xPBS, followed by detachment with 1xTrypsin. Cells were resuspended with fresh media and centrifuged at 1000 rpm for 5 minutes. The freezing media containing 50% FBS and 10% DMSO (Sigma 41639-500ml) was prepared. After centrifugation, the pellet was resuspended in the freezing media to break the pellet. The cell suspension was then distributed to cryovials and frozen at -80°C.

Cell counting

The cell passaging protocol was followed: aspirating media, washing with 1xPBS, and trypsinization. Then, cells were resuspended in a complete medium, and 10µl of the suspension was pipetted onto one chamber of a hemocytometer. Cells were counted in 4 squares out of 16. The formula below was used to calculate the number of cells:

$$\text{Cell count per mL} = \frac{\text{Number of Cells Counted}}{\text{Number of Corner Squares counted}} \times \text{Dilution factor} \times 10,000$$

Condition media collection

Cells were first cultured in the adjusted RPMI media with 10% FBS. Media was then changed to serum-free with the exact composition of penicillin, non-essential amino acids, and sodium pyruvate, as described earlier. After incubation for 24 hours in serum-free RPMI, the conditioned medium was collected and processed.

Conditioned media were spun down at 1000 rpm at 23°C for 5 minutes to pellet cell debris. Following centrifugation, the supernatant was concentrated using Sartorius Vivaspin™ Turbo 15 Regenerated Cellulose (RC) ultrafiltration centrifugal concentrator with a 10 000 kDa molecular weight cutoff.

Lysates preparation

After removing media, cells were rinsed with 1xPBS 2-3 times, followed by adding 1xLaemmli Buffer: 1ml to T75 flask, 150µl to one well of a 6-well plate. Cells were then detached by a cell scraper and collected into an Eppendorf tube. To lyse concentrated conditioned media, 100µl of 10xEDTA, 100µl 10xProtease cocktail, and 250µl 4xLaemmli Buffer were added.

Western blotting

Protein lysates

Cells were grown until 70-80% confluent on a 6 cm² Petri dish or until the experiment was complete on a 6-well plate. Media were removed, and cells were washed with 1xPBS. Cells were then lysed by adding 150 µl of 1xLaemmli Buffer. After scraping the surface of a plate, lysed cells were collected into 1 ml Eppendorf tubes. For protein analysis, lysates were heated to 94°C for 5 minutes and cooled to room temperature. Lysates were then sonicated (SoniPrep 150, MSE) at 14 µm for 15 seconds three times to shear the DNA. Afterward, the protein lysates were combined with 6µl of protein loading solution, which is a mixture of 1% Bromophenol and 100% β Mercaptaethanol at a 1:1 ratio. The resulting mixture was then stored at -20°C.

Sodium Dodecyl Sulphate-Polyacrylamide Gel Electrophoresis (SDS-PAGE)

The SDS-PAGE method was used to analyze the expression of target proteins. 8% and 10% resolving gel were prepared for different analyses (See Table 2). After assembling glass plates, the resolving gel was poured in and left to solidify for 15 minutes. The preparation of the stacking gel involved combining water, 30% acrylamide solution, 1.0 M Tris (pH 6.8), 10% APS, and TEMED. This mixture was then added onto the top of the resolving gel. At the same time, a 10 or 15-well comb was inserted into the stacking gel, and the gel was left to solidify for 15 minutes. Once the gel had been ready, it was placed in a tank, and a 1xRunning buffer was poured on top of it until a corresponding mark. Loading samples were boiled at 94°C for 5 minutes and were then added by 15 µl to the gel. A protein ladder (PageRuler™, #26619) was added by 4 µl. The running was conducted at 120V for 1.5 hours.

Table 2. Resolving gel components

% Gel	Water (ml)	30% Acrylamide solution (ml)	1.5M Tris pH 8.8 (ml)	10% SDS (ml)	10% APS	TEMED
8	6.9	4.0	3.8	0.15	0.15	0.009
10	5.9	5.0	3.8	0.15	0.15	0.006

Transferring the SDS-PAGE gel to the PVDF membrane

After SDS-PAGE running, proteins were transferred to the PVDF membrane (Immobilon-P, Millipore, IPVH 00010). The cassette was assembled as illustrated in Figure 4. Meanwhile, the membrane was activated in ethanol for 5 minutes. Then, the assembled cassette was inserted into a tank with 1xTransfer Buffer, and the power was set at 20V for 18 hours.

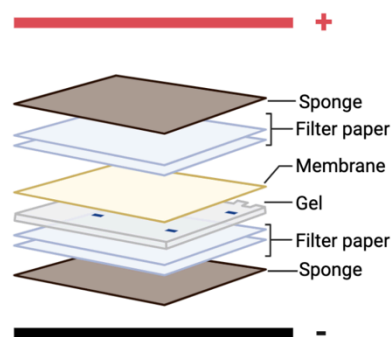


Figure 4. Transfer cassette assembly. Adapted from “Icon Pack - Gel Electrophoresis”, by BioRender.com (2023). Retrieved from <https://app.biorender.com/biorender-templates>.

Blocking and antibody incubation

After the electrotransfer, the membrane was stained with 0.1% Ponceau S solution for 10 minutes to check the protein transfer efficiency. Then, it was washed with distilled water three times to clean the membrane from the stain. For blocking, the membrane was placed in a plastic tray

containing 20 ml TBS-T-milk for 1 hour. The membrane was then washed with TBS-T three times for 5 minutes before incubation with primary antibodies for 1 hour at room temperature. The same washing step was repeated before incubation with secondary antibodies for 1 hour at room temperature. See Tables 3 and 4 to check the antibodies used in the study.

The protein expression levels were visualized by incubating the membrane in the Pierce ECL substrate kit (solution A and B at 1:1 ratio) for 5 minutes and using The ChemiDoc MP Imaging System.

Table 3. Description of primary antibodies.

Antibody	Type	Host	Dilution	Company
AXL	Polyclonal	Goat	1:5000	R&D
Tubulin	Monoclonal	Mouse	1:150 000	Sigma
pAkt - 473	Monoclonal	Rabbit	1:2000	Cell Signaling
pAXL - 702	Polyclonal	Rabbit	1:2000	Invitrogen
pAkt - 308	Monoclonal	Rabbit	1:1000	Cell Signaling
p44/42 MAPK (Erk1/2)	Monoclonal	Rabbit	1:2000	Cell Signaling

Table 4. Description of secondary antibodies.

Antibody	Type	Host	Dilution	Company
Anti-Goat IgG/HRP	Polyclonal	Rabbit	1:5000	Abcam
Anti-Mouse IgG/HRP	Polyclonal	Goat	1:5000	Abcam
Anti-Rabbit IgG/HRP	Polyclonal	Goat	1:3000	Abcam

Experimental Design

Two separate experiments were conducted.

Experiment I. Examination of toxicity of the recombinant AXL protein.

J82 and HT1376 cells were seeded into 6-well plates by 3×10^5 and 5×10^5 cells/well, respectively. Cells were first cultured with RPMI (10% FBS) medium for 24 hours. The recombinant AXL protein (Sino Biological, Inc., #10279-H08H) was added at different concentrations (100, 10, 1 ng/ml, and 100 pg/ml in 2 ml serum-free RPMI). In addition, cells were cultured in 2 ml of serum-containing and serum-free RPMI media for controls. The plates were then incubated at 37°C for 24 hours, and cells were imaged under an inverted light microscope. Finally, cells were lysed.

Experiment II. Treatment with recombinant AXL and Gas 6.

This experiment was conducted over 4 days. On day 1, cells were seeded and cultured the same way as in the previous experiment. On day 2, cells were starved in a serum-free medium for another 24 hours. The media in each well was changed on the third day, according to Figure 5. The next day, well 3B (in Figure 5) was treated with recombinant AXL for 1 hour. At all steps, wells were imaged before and after (0, 1.5 hours) treatment with AXL. Following the treatment with AXL on day 4, wells 2B, 3A, and 3B were treated with recombinant Gas6 protein (R&D Systems, #885-GSB-050).

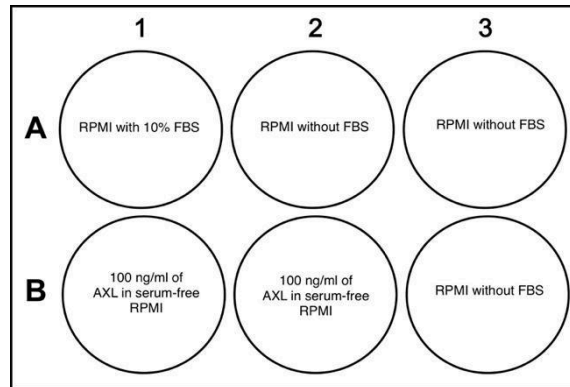


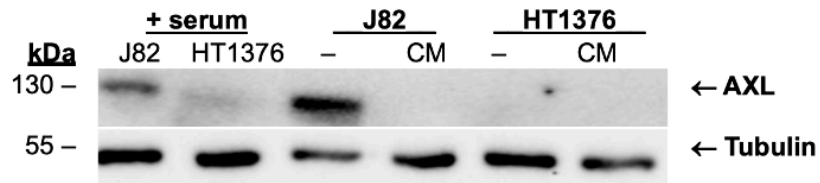
Figure 5. Schematic representation of the experiment. All wells were filled with 2 ml of the indicated media.

Results

AXL expression in bladder cancer cell lines

We examined the expression of AXL in positive and negative cell lines: J82 and HT1376, respectively (Figure 6). AXL was expressed in J82 cells cultured in both media, with and without serum. As expected, it was absent in HT1376 cells. In addition, there was soluble AXL expression in the condition media of AXL-positive J82 cells, while it was absent in HT1376 condition media.

A



B

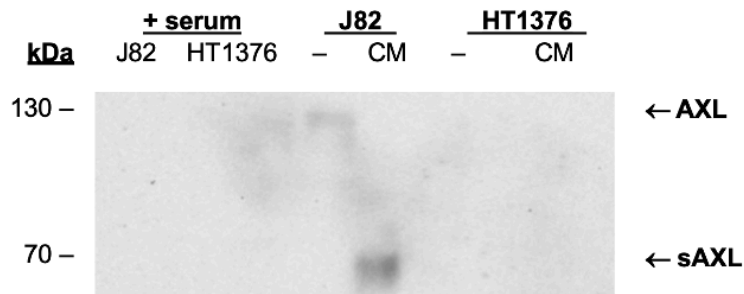


Figure 6. (A) Expression of AXL, Tubulin, and (B) sAXL in J82 and HT1376 bladder cancer cells. Abbreviations: “+ serum” represents lysates of cells that were cultured media with 10% FBS; “-” - cells grown in media without FBS; CM - conditioned media.

Validation of the recombinant AXL

The recombinant AXL protein product was attested before the experiments were started. Western blot analysis revealed that the molecular weight cutoff was around 70 kDa (Figure 7). According to the manufacturer’s recommendation, the 0.25 $\mu\text{g/ml}$ stock solution was prepared. The original Axl solution was diluted to 20 $\text{ng}/\mu\text{l}$ with further dilution to 100 ng/ml , 10 ng/ml , 1 ng/ml , and 100 pg/ml for follow-up experiments.

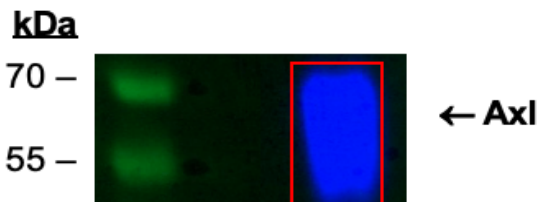


Figure 7. Validation of the recombinant AXL protein by western blot.

Toxicity of the recombinant AXL on J82 and HT1376 cells

Different protein concentrations were added to investigate the toxicity of the recombinant AXL (Figure 8). The result showed that the recombinant protein is not toxic for J82 cells after overnight incubation.

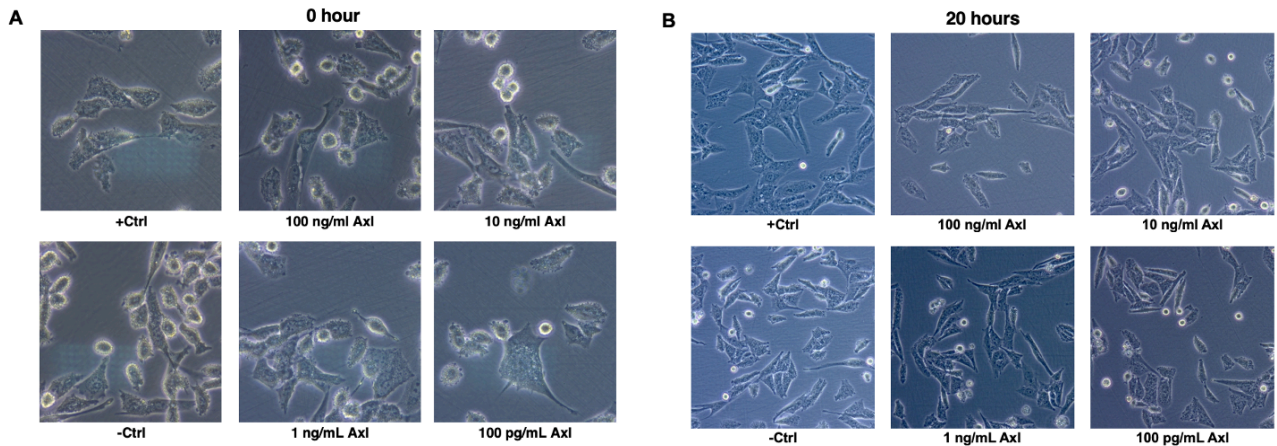


Figure 8. Representative images of the J82 cells, treated with different concentrations of recombinant AXL. (A) shows images at 0 hour after the treatment. (B) Images after overnight incubation with AXL. Abbreviations: +Ctrl – media with serum; -Ctrl – media without serum.

Analysis of the recombinant AXL effect on cells

J82 and HT1376 cells were grown in media with serum with further one-day starvation. After cells were starved, 100 ng/mL of AXL was added to investigate its effect on positive and negative cell lines. This concentration was chosen because it is close to the amount of soluble AXL found in cancer patients. It can be seen from Fig. 9A and 9C that the recombinant AXL affects cell-to-cell communication and attachment of J82 and HT1376 bladder cancer cells. The most prominent phenotypic difference was observed after 1-hour incubation with the protein for both cell lines. In particular, HT1376 cells showed a change in cell-to-cell communication by expressing more protrusions. There was an alteration in the adhesion of J82 cells, with them being flatter and wider. Fig. 9B and 9D show cells before and after incubation with Gas6. Phenotypic differences were indistinguishable.

Investigation of downstream signaling

Western blot analysis was performed to find whether the recombinant AXL affects the activity of downstream signaling pathways. AXL was expressed in all J82 cells except for cells treated with AXL for 1 hour and Gas6 for 10 minutes (Figure 10A). Tubulin was used as a control and was evenly expressed in both HT1376 and J82 cells, illustrating accurate loading (Fig.10A).

Figure 10B shows the presence of phospho-AXL at Y702 and Y779. In HT1376 cells, the AXL receptor is absent; therefore, western blot analysis indicates the expression of receptors at similar sites. Namely, phosphorylation at Y702 is upregulated with AXL +Gas6 addition. Incubation with Gas6 merely changes the expression of pAXL-702, while the recombinant AXL treatment for 24 hours upregulates it. Gas6 also stimulates the phosphorylation of AXL at Y779 on its own and in the complex with AXL.

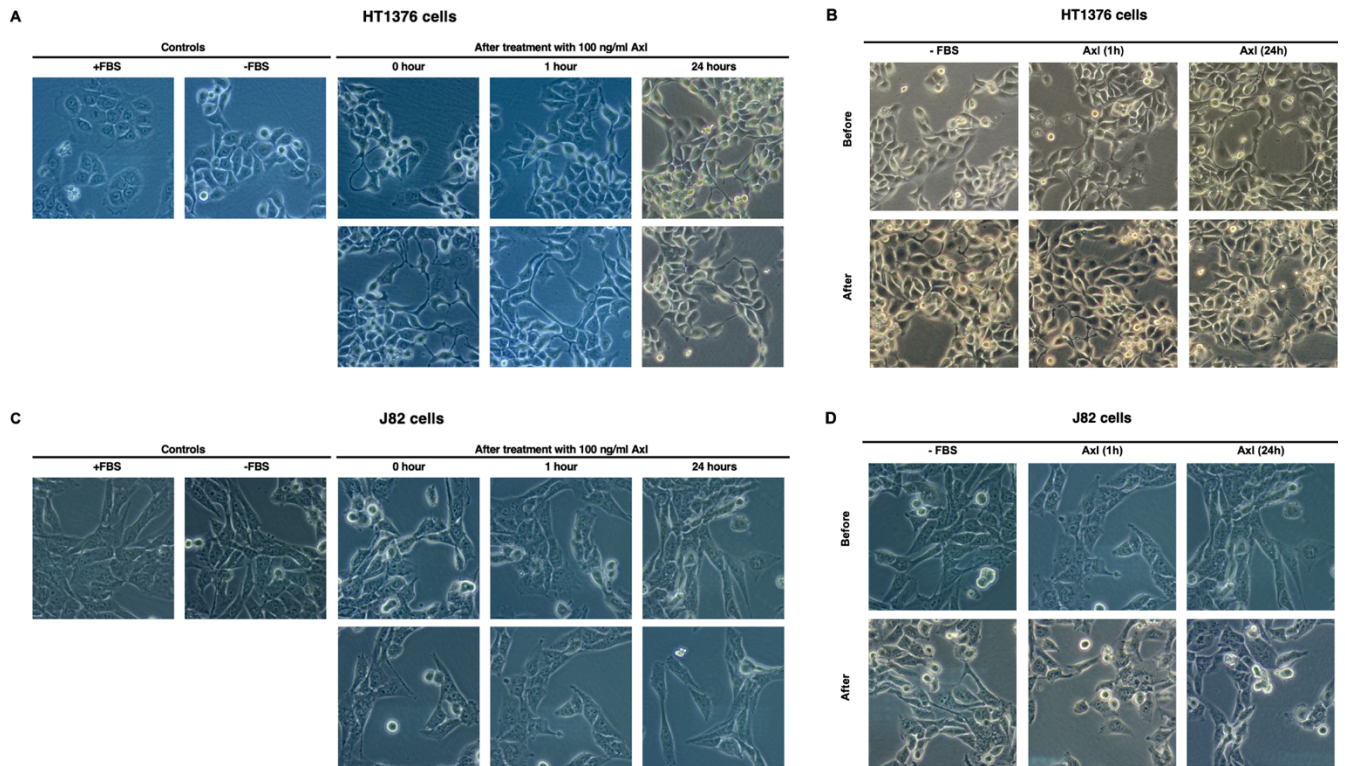


Figure 9. Representative images of cells after treatment with AXL and Gas6. (A) HT1376 and (C) J82 cells after treatment with 100 ng/ml AXL at 0, 1, and 24 h. (B) HT1376 and (D) J82 cells before and after incubation with Gas6 for 10 min. Abbreviations: FBS - fetal bovine serum.

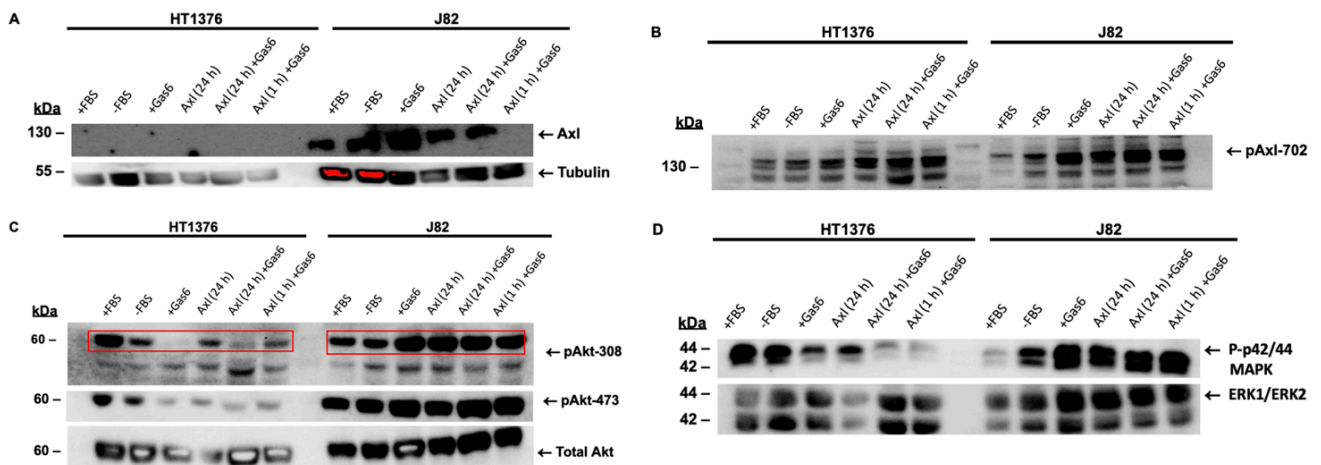


Figure 10. Different proteins expression in HT1376 and J82 cells after treatment with AXL and Gas6.

AXL-positive J82 cells have different pAXL expressions. Incubations with Gas6, AXL (24h) +Gas6, AXL (1h) +Gas6 have a similar extent of AXL activation at Y702; in comparison, there is slightly less upregulation of pAXL-702 by AXL (24h). The results of pAXL-779 in J82 cells cannot be interpreted due to some damage to the membrane.

Next, expressions of downstream targets, Akt and MAPK, were analyzed (Figures 10C and D). In HT1376 cells, pAkt-308 was inhibited by Gas6. However, the downregulation of Akt-308

activation was less when treated with the Gas6-AXL complex. Particularly, pAkt-308 expression was close to control in cells where Gas6 was added after 1-hour AXL incubation. Gas6 also suppresses pAkt-473, and a similar effect is noticeable with AXL incubation. Yet, when cells were treated with AXL (24h) alone or with Gas6-AXL(1h) complex, there was slightly higher expression of pAkt-473. It is hard to interpret total Akt expression accurately due to prolonged exposure to the membrane. Nevertheless, the amount of total AXL is approximately the same.

In J82 cells, Akt phosphorylation at Thr308 was upregulated by all of the performed treatments. In particular, it was upregulated when Gas6 and AXL were added solely and combined. Phosphorylation of Akt-473 was upregulated in cells incubated with Gas6 and AXL (24h/1h) +Gas6, while it was not changed in cells treated with only AXL for 24h. The same effect of upregulation can be observed in total-Akt expression: Gas6 and Gas6-AXL complex increases it, with the latter giving a stronger effect.

Regarding activation of p44/42 MAPK (Erk1/2), incubation of HT1376 cells with Gas6 or AXL (24h) has a similar extent of downregulation. Meanwhile, phosphorylation of p44/42 occurs significantly less in cells treated with Gas6+AXL. The total p44/42 is less affected by Gas6 and Gas6+AXL incubation. Nevertheless, it is less expressed in cells with the recombinant AXL treatment for 24 hours. In Axl-positive J82 cells, phosphorylation of p44/42 is upregulated by Gas6, AXL, and Gas6+ AXL incubation. The same effect was observed in total Erk1/2 expression.

Discussion

The AXL receptor tyrosine kinase is a promising target for cancer therapy because its excessive presence has been reported to be closely linked to the development of metastasis across different types of cancers, such as lung, breast, ovarian, and pancreatic carcinoma (Auyez et al., 2021). Only a limited number of studies examined the correlation between the progression of bladder cancer and the expression of AXL (Wang et al., 2019). As per the soluble form of the receptor, there is currently no information in this context. Therefore, this capstone project investigates the role of soluble AXL in bladder cancer cells.

According to preliminary data (received by Almira Auyez), soluble AXL is present in urine samples of cancer patients and healthy controls. These findings raised the question of whether sAXL has a functional role in bladder cancer cells or appears as an indication of the receptor's work. This study analyzes two bladder cancer cell lines - HT1376 (AXL negative) and J82 (AXL positive). The idea of the experiments was to examine the effect of soluble AXL on cell behavior and downstream signaling pathways and test the hypothesis on sAXL's function as a decoy receptor.

At first, AXL expression in bladder cancer cell lines was analyzed. Overexpression of AXL was observed in J82 cells. At the same time, there was little or no expression of AXL in HT1376 cell lines (Figure 6). Figure 6 also shows that soluble AXL is present in the conditioned media of J82 cells at approximately 70 kDa. These results are consistent with the reports conducted by EMT group members (Ilona Malikova and Aiya Chukanova). It should be considered that the excessive expression of AXL has been identified in cells with mesenchymal properties, which are considered to be highly metastatic. In contrast, HT1376 cells, which are negative to AXL, express epithelial phenotype and are less aggressive. Thus, AXL expression correlates with cancer progression.

Epithelial-Mesenchymal Transition (EMT) is a cellular process during which cell-cell and cell-extracellular matrix interactions are altered, leading to the detachment of epithelial cells. It results in a new transcriptional program that promotes cells to acquire mesenchymal phenotypes and behavior and downregulate epithelial features. EMT leads to increased tumor-initiating metastatic potential and resistance to therapies in the context of cancer. It was reported that overexpression of AXL is responsible for inducing EMT through direct regulation of EMT markers such as E-, N-Cadherin, Snail, and Slug (Asiedu et al.). In this study, the recombinant AXL was added to AXL-negative and Axl-positive cells, which were imaged after the treatment. In HT1376 cells, the addition of AXL protein increased the formation of protruding filopodia. As indicated previously, the overexpression of AXL is significantly linked to changes in cell morphology, specifically, transition to mesenchymal phenotypes resulting in an upregulated cell migration (Gjerdrum et al., 2010 & Lay et al., 2007). Thus, changes seen in 6A can be a direct effect of the recombinant AXL and may be the result of EMT induction. In J82 cells, there is a different phenotypic change in the appearance of cells. They become wider and flatter and are more spread on the surface. Recent studies showed that AXL promotes the phosphorylation of the focal adhesion protein network, making focal adhesion disassembly faster (Abu-Thuraia et al.). The altered appearance of J82 cells after treatment with AXL may be a result of the stimulated focal adhesion dynamics.

It is important to mention that in both cells, positive and negative, the most notable changes were seen after 1-hour incubation with the recombinant. After 24 hours of treatment, changes were

less significant; therefore, it indicated that the experiment could have been stopped after 1 hour, and cells needed to be lysed.

The binding of Gas6 to the AXL receptor causes its dimerization and cross-phosphorylation, which triggers a cascade of signaling pathways. As observed in three-dimensional structures of the AXL and Gas6 complex, the C-terminus laminin G-type 1 domain of Gas6 binds to the Ig domains of AXL (Sasaki et al., 2006). It was revealed that Gas6 binds to sAXL with high affinity and leads to the inhibition of ligand-mediated activation of AXL (Hafizi & Dahlbäck, 2006b). To investigate whether soluble AXL affects downstream signaling and acts as a decoy receptor, Gas6 was added to cells for 10 minutes after treatment with the recombinant AXL. Phenotypically, cells were not changed much.

To establish if AXL is activated, the phosphorylation level of AXL was assessed through Western blotting. Overall, incubation with AXL for 24 hours has similar effects on cells as when it is in complex with Gas6. Moreover, it is important to note that pAXL antibodies can detect other phospho-TAM receptors due to close phosphorylation sites (see Figure 1). In Fig.3, other bands may represent Mer or Tyro3 receptors activation. For instance, a protein at lower than 130kDa in pAx1-702 is upregulated with the addition of AXL (24h) + Gas6, while other wells show no change. It may indicate that the recombinant AXL interacts with other receptors and leads to similar activation of TAMs. Considering that HT1376 cells are negative for AXL, it is obvious that other receptors (TYRO3 or MERTK) were detected by western blotting and were affected by the recombinant AXL. In this instance, according to Korshunov (2011), there is still a limited understanding of the functional interactions of AXL with other TAM receptors. Based on the gene co-expression profile of TAM receptors, it has been suggested that the AXL homodimer can form heterodimers with TYRO3 or MERTK. Nonetheless, there is no experimental data on the heterodimerization of TAM RTKs. In his paper, Korshunov (2011) highlights an earlier study conducted by Bellosta et al. (1995) where was revealed that AXL can undergo homophilic binding and this interaction does not require its intracellular domain. In insects, specific interactions between AXL-expressing cells increase cell aggregation. Such ligand-independent activation is caused by experimental overexpression of AXL. A similar interaction may have occurred in the present experiment; thus, the AXL-AXL interaction was driven by the recombinant protein causing the same effect on J82 cells as a ligand-dependent activation.

Activation of TAMs upon ligand-dependent or ligand-independent interaction sets off a cascade of different signaling pathways. To this end, phospho- and total Akt and MAPK were analyzed via western blotting. In general, AXL-negative and AXL-positive cells have an opposite expression of downstream targets upon incubation with Gas6. For instance, pAkt expression is downregulated in HT1376 cells and upregulated in J82 cells. The exact correlation is observed in the expression of phospho-p42/44. In both cell lines, the recombinant AXL leads to similar activation/inactivation of downstream signaling targets, as does Gas6 incubation. It may indicate that the recombinant AXL interacts with TAMs or other receptors similarly to Gas6. Nevertheless, there was one exceptional result where the recombinant AXL acts as a decoy receptor to Gas6 in the phosphorylation of Akt at Thr308 in HT1376 cells.

One reason for the recombinant AXL not being a decoy receptor in the conducted experiments may be an excess of Gas6. In this study, Gas6 concentration exceeded AXL's because we did not know whether the ligand was active. Therefore, in the future, adding the recombinant

Gas6 and AXL in a similar amount is recommended. It was also decided that Gas6 and AXL should be pre-incubated before adding to cells to ensure their binding.

In conclusion, the present study reports an interesting finding that recombinant AXL elicits a similar downstream signaling pathway response as Gas6 in bladder cancer cells. However, the hypothesis that soluble AXL is a decoy receptor remains unresolved since, in Akt activation, it inhibits the Gas6 effect, while in other interactions, it upregulates the signal or has no effect. The main limitation of this study is the absence of repetitions; thereby the results may not be representative and require additional experiments to confirm the findings. For further analysis, the experimental design needs to undergo changes such as a ligand-receptor pre-incubation and conducting an experiment for 1-1.5 hours rather than 24 hours. Future studies should examine possible interactions between soluble AXL and TAM receptors and uncover underlying molecular mechanisms.

References

- Abboud-Jarrous, G., Priya, S., Maimon, A., Fischman, S., Cohen-Elisha, M., Czerninski, R., & Burstyn-Cohen, T. (2017). Protein S drives oral squamous cell carcinoma tumorigenicity through regulation of axl. *Oncotarget*, 8(8), 13986–14002.
<https://doi.org/10.18632/oncotarget.14753>
- Antony, J., & Huang, R. Y.-J. (2017). Axl-driven EMT State as a targetable conduit in cancer. *Cancer Research*, 77(14), 3725–3732. <https://doi.org/10.1158/0008-5472.can-17-0392>
- Asiedu, M., Beauchamp-Perez, F., Ingle, J. et al. AXL induces epithelial-to-mesenchymal transition and regulates the function of breast cancer stem cells. *Oncogene* 33, 1316–1324 (2014).
<https://doi.org/10.1038/onc.2013.57>
- Auyez, A., Sayan, A. E., Kriajevskaja, M., & Tulchinsky, E. (2021). Axl receptor in cancer metastasis and drug resistance: When normal functions go Askew. *Cancers*, 13(19), 4864.
<https://doi.org/10.3390/cancers13194864>
- Bellosta, P., Costa, M., Lin, D. A., & Basilico, C. (1995). The receptor tyrosine kinase ark mediates cell aggregation by homophilic binding. *Molecular and Cellular Biology*, 15(2), 614–625. <https://doi.org/10.1128/mcb.15.2.614>
- Budagian, V., Bulanova, E., Orinska, Z., Duitman, E., Brandt, K., Ludwig, A., Hartmann, D., Lemke, G., Saftig, P., & Bulfone-Paus, S. (2005). Soluble axl is generated by ADAM10-dependent cleavage and associates with gas6 in mouse serum. *Molecular and Cellular Biology*, 25(21), 9324–9339. <https://doi.org/10.1128/mcb.25.21.9324-9339.2005>
- Dougherty, D. W., Gonsorcik, V. K., Harpster, L. E., Trussell, J. C., & Drabick, J. J. (2009). Superficial bladder cancer metastatic to the lungs: Two case reports and review of the literature. *Urology*, 73(1). <https://doi.org/10.1016/j.urology.2008.01.050>

- Dreicer, R. (2017). Chemotherapy for advanced urothelial cancer: End of the beginning? *The Lancet Oncology*, 18(5), 567–569. [https://doi.org/10.1016/s1470-2045\(17\)30241-3](https://doi.org/10.1016/s1470-2045(17)30241-3)
- Du, Z., & Lovly, C. M. (2018). Mechanisms of receptor tyrosine kinase activation in cancer. *Molecular Cancer*, 17(1). <https://doi.org/10.1186/s12943-018-0782-4>
- Flem Karlsen, K.; McFadden, E.; Florenes, V.A.; Davidson, B. Soluble AXL is ubiquitously present in malignant serous effusions. *Gynecol. Oncol.* 2019, 152, 408–415.
- Gjerdrum, C., Tiron, C., Høiby, T., Stefansson, I. M., Haugen, H., Sandal, T., Collett, K., Li, S., McCormack, E., Gjertsen, B. T., Micklem, D., Akslén, L. A., Glackin, C. A., & Lorens, J. B. (2010). Axl is an essential epithelial-to-mesenchymal transition-induced regulator of breast cancer metastasis and patient survival. *Proceedings of the National Academy of Sciences of the United States of America*, 107(3), 1124–1129. <https://doi.org/10.1073/pnas.0909333107>
- Hafizi, S., & Dahlbäck, B. (2006a). Gas6 and protein S. *FEBS Journal*, 273(23), 5231–5244. <https://doi.org/10.1111/j.1742-4658.2006.05529.x>
- Hafizi, S., & Dahlbäck, B. (2006b). Signalling and functional diversity within the AXL subfamily of receptor tyrosine kinases. *Cytokine & Growth Factor Reviews*, 17(4), 295–304. <https://doi.org/10.1016/j.cytogfr.2006.04.004>
- Janssen JW;Schulz AS;Steenvoorden AC;Schmidberger M;Strehl S;Ambros PF;Bartram CR; (n.d.). A novel putative tyrosine kinase receptor with oncogenic potential. *Oncogene*. Retrieved March 19, 2023, from <https://pubmed.ncbi.nlm.nih.gov/1834974/>
- Kamat, A. M., Hahn, N. M., Efstathiou, J. A., Lerner, S. P., Malmström, P.-U., Choi, W., Guo, C. C., Lotan, Y., & Kassouf, W. (2016). Bladder cancer. *The Lancet*, 388(10061), 2796–2810. [https://doi.org/10.1016/s0140-6736\(16\)30512-8](https://doi.org/10.1016/s0140-6736(16)30512-8)
- Kariolis MS, Miao YR, Jones DS 2nd, Kapur S, Mathews GAJ II, Cochran JR. An engineered Axl ‘decoy receptor’ effectively silences the Gas6-Axl signaling axis. *Nat Chem Biol.* 2014;10(11):977–83.

- Karl, K., Light, T. P., & Hristova, K. (2022). Receptor tyrosine kinases. *Comprehensive Pharmacology*, 10–36. <https://doi.org/10.1016/b978-0-12-820472-6.00135-3>
- Korshunov, V. A. (2011). Axl-dependent signalling: A clinical update. *Clinical Science*, 122(8), 361–368. <https://doi.org/10.1042/cs20110411>
- Lay, J.-D., Hong, C.-C., Huang, J.-S., Yang, Y.-Y., Pao, C.-Y., Liu, C.-H., Lai, Y.-P., Lai, G.-M., Cheng, A.-L., Su, I.-J., & Chuang, S.-E. (2007). Sulfasalazine suppresses drug resistance and invasiveness of lung adenocarcinoma cells expressing axl. *Cancer Research*, 67(8), 3878–3887. <https://doi.org/10.1158/0008-5472.can-06-3191>
- Lemke, G. (2013). Biology of the TAM Receptors. *Cold Spring Harbor Perspectives in Biology*, 5(11), a009076. <https://doi.org/10.1101/cshperspect.a009076>
- Lemmon, M. A., & Schlessinger, J. (2010). Cell signaling by receptor tyrosine kinases. *Cell*, 141(7), 1117–1134. <https://doi.org/10.1016/j.cell.2010.06.011>
- Lew, E. D., Oh, J., Burrola, P. G., Lax, I., Zagórska, A., Través, P. G., Schlessinger, J., & Lemke, G. (2014). Differential Tam receptor–ligand–phospholipid interactions delimit differential TAM bioactivities. *ELife*, 3. <https://doi.org/10.7554/elife.03385>
- Liu, E., Hjelle, B., & Bishop, J. M. (1988). Transforming genes in chronic myelogenous leukemia. *Proceedings of the National Academy of Sciences*, 85(6), 1952–1956. <https://doi.org/10.1073/pnas.85.6.1952>
- Martin-Doyle, W., & Kwiatkowski, D. J. (2015). Molecular biology of bladder cancer. *Hematology/Oncology Clinics of North America*, 29(2), 191–203. <https://doi.org/10.1016/j.hoc.2014.10.002>
- Martínez-Bosch, N., Cristóbal, H., Iglesias, M., Gironella, M., Barranco, L., Visa, L., Calafato, D., Jiménez-Parrado, S., Earl, J., Carrato, A., Manero-Rupérez, N., Moreno, M., Morales, A., Guerra, C., Navarro, P., & García de Frutos, P. (2022). Soluble AXL is a novel blood marker for early detection of pancreatic ductal adenocarcinoma and differential diagnosis from

chronic pancreatitis. *EBioMedicine*, 75, 103797.

<https://doi.org/10.1016/j.ebiom.2021.103797>

- Miller, M. A., Oudin, M. J., Sullivan, R. J., Wang, S. J., Meyer, A. S., Im, H., Frederick, D. T., Tadros, J., Griffith, L. G., Lee, H., Weissleder, R., Flaherty, K. T., Gertler, F. B., & Lauffenburger, D. A. (2016). Reduced proteolytic shedding of receptor tyrosine kinases is a post-translational mechanism of kinase inhibitor resistance. *Cancer Discovery*, 6(4), 382–399. <https://doi.org/10.1158/2159-8290.cd-15-0933>
- Oliveira, M. C., Caires, H. R., Oliveira, M. J., Fraga, A., Vasconcelos, M. H., & Ribeiro, R. (2020). Urinary biomarkers in bladder cancer: Where do we stand and potential role of extracellular vesicles. *Cancers*, 12(6), 1400. <https://doi.org/10.3390/cancers12061400>
- O'Bryan, J. P., Frye, R. A., Cogswell, P. C., Neubauer, A., Kitch, B., Prokop, C., Espinosa, R., Le Beau, M. M., Earp, H. S., & Liu, E. T. (1991). Axl, a transforming gene isolated from primary human myeloid leukemia cells, encodes a novel receptor tyrosine kinase. *Molecular and Cellular Biology*, 11(10), 5016–5031. <https://doi.org/10.1128/mcb.11.10.5016-5031.1991>
- Pacez, J. D., Vogelsang, M., Parker, M. I., & Zerbini, L. F. (2013). The receptor tyrosine kinase axl in cancer: Biological Functions and Therapeutic Implications. *International Journal of Cancer*, 134(5), 1024–1033. <https://doi.org/10.1002/ijc.28246>
- Rankin, E. B., Fuh, K. C., Taylor, T. E., Krieg, A. J., Musser, M., Yuan, J., Wei, K., Kuo, C. J., Longacre, T. A., & Giaccia, A. J. (2010, September 29). Axl is an essential factor and therapeutic target for metastatic ovarian cancer. *American Association for Cancer Research*. Retrieved March 19, 2023, from <https://doi.org/10.1158/0008-5472.can-10-1267>
- Sadahiro, H.; Kang, K.D.; Gibson, J.T.; Minata, M.; Yu, H.; Shi, J.; Chhipa, R.; Chen, Z.; Lu, S.; Simoni, Y.; et al. Activation of the Receptor Tyrosine Kinase AXL Regulates the Immune Microenvironment in Glioblastoma. *Cancer Res.* 2018, 78, 3002–3013.

- Saginala, K., Barsouk, A., Aluru, J. S., Rawla, P., Padala, S. A., & Barsouk, A. (2020).
Epidemiology of Bladder Cancer. *Medical Sciences*, 8(1), 15.
<https://doi.org/10.3390/medsci8010015>
- Schneider, C., King, R. M., & Philipson, L. (1988). Genes specifically expressed at growth arrest of mammalian cells. *Cell*, 54(6), 787–793. [https://doi.org/10.1016/s0092-8674\(88\)91065-3](https://doi.org/10.1016/s0092-8674(88)91065-3)
- Sung, H., Ferlay, J., Siegel, R. L., Laversanne, M., Soerjomataram, I., Jemal, A., & Bray, F. (2021). Global cancer statistics 2020: Globocan estimates of incidence and mortality worldwide for 36 cancers in 185 countries. *CA: A Cancer Journal for Clinicians*, 71(3), 209–249.
<https://doi.org/10.3322/caac.21660>
- Verma, A., Warner, S. L., Vankayalapati, H., Bearss, D. J., & Sharma, S. (2011). Targeting axl and Mer kinases in cancer. *Molecular Cancer Therapeutics*, 10(10), 1763–1773.
<https://doi.org/10.1158/1535-7163.mct-11-0116>
- Wang C., Jin H., Wang N., Fan S., Wang Y., Zhang Y., Wei L., Tao X., Gu D., Zhao F., et al.
Gas6/Axl Axis Contributes to Chemoresistance and Metastasis in Breast Cancer through Akt/GSK-3beta/beta-catenin Signaling. *Theranostics*. 2016;6:1205–1219. doi: 10.7150/thno.15083.
- Wang, L., Liu, K., Yu, J., & Sun, E. (2019). A retrospective analysis of the correlation between AXL expression and clinical outcomes of patients with urothelial bladder carcinoma. *Translational Cancer Research*, 8(3), 976–984. <https://doi.org/10.21037/tcr.2019.06.06>
- Wu, X., Liu, X., Koul, S., Lee, C. Y., Zhang, Z., & Halmos, B. (2014). Axl kinase as a novel target for cancer therapy. *Oncotarget*, 5(20), 9546–9563. <https://doi.org/10.18632/oncotarget.2542>
- Zangouei, A. S., Barjasteh, A. H., Rahimi, H. R., Mojarrad, M., & Moghbeli, M. (2020). Role of tyrosine kinases in Bladder Cancer Progression: An overview. *Cell Communication and Signaling*, 18(1). <https://doi.org/10.1186/s12964-020-00625-7>

Zhu, C., Wei, Y. & Wei, X. AXL receptor tyrosine kinase as a promising anti-cancer approach: functions, molecular mechanisms and clinical applications. *Mol Cancer* 18, 153 (2019).
<https://doi.org/10.1186/s12943-019-1090-3>